frontiers | Frontiers in Neural Circuits

TYPE Original Research
PUBLISHED 29 August 2024
DOI 10.3389/fncir.2024.1448592

OPEN ACCESS

EDITED BY
Kensaku Mori,
RIKEN,'Japan

REVIEWED BY
Shin Nagayama,
Texas Medical Center, United States
Jackson Cioni Bittencourt,
University of São Paulo, Brazil

*CORRESPONDENCE
Hajime Suyama
✉ hajime.suyama@ovgu.de

†PRESENT ADDRESS
Hajime Suyama,
Institute of Biology, Otto-von-Guericke University Magdeburg, Magdeburg, Germany

RECEIVED 13 June 2024
ACCEPTED 13 August 2024
PUBLISHED 29 August 2024

CITATION
Suyama H, Bianchini G and Lukas M (2024) Vasopressin differentially modulates the excitability of rat olfactory bulb neuron subtypes.
Front. Neural Circuits 18:1448592.
doi: 10.3389/fncir.2024.1448592

Vasopressin differentially modulates the excitability of rat olfactory bulb neuron subtypes

Hajime Suyama[1]*†, Gaia Bianchini[2] and Michael Lukas[1]

[1]Institute of Zoology, Neurophysiology, University of Regensburg, Regensburg, Germany, [2]Neural Circuits and Behavior Laboratory, The Francis Crick Institute, London, United Kingdom

Vasopressin (VP) plays a crucial role in social memory even at the level of the olfactory bulb (OB), where OB VP cells are activated during social interactions. However, it remains unclear how VP modulates olfactory processing to enable enhanced discrimination of very similar odors, e.g., rat body odors. Thus far, it has been shown that VP reduces firing rates in mitral cells (MCs) during odor presentation *in vivo* and decreases the amplitudes of olfactory nerve-evoked excitatory postsynaptic potentials (ON-evoked EPSPs) in external tufted cells *in vitro*. We performed whole-cell patch-clamp recordings and population Ca^{2+} imaging on acute rat OB slices. We recorded ON-evoked EPSPs as well as spontaneous inhibitory postsynaptic currents (IPSCs) from two types of projection neurons: middle tufted cells (mTCs) and MCs. VP bath application reduced the amplitudes of ON-evoked EPSPs and the frequencies of spontaneous IPSCs in mTCs but did not change those in MCs. Therefore, we analyzed ON-evoked EPSPs in inhibitory interneurons, i.e., periglomerular cells (PGCs) and granule cells (GCs), to search for the origin of increased inhibition in mTCs. However, VP did not increase the amplitudes of evoked EPSPs in either type of interneurons. We next performed two-photon population Ca^{2+} imaging in the glomerular layer and the superficial GC layer of responses to stronger ON stimulation than during patch-clamp experiments that should evoke action potentials in the measured cells. We observed that VP application increased ON-evoked Ca^{2+} influx in juxtaglomerular cells and GC somata. Thus, our findings indicate inhibition by VP on projection neurons via strong ON input-mediated inhibitory interneuron activity. This neural modulation could improve representation of odors, hence, better discriminability of similar odors, e.g., conspecific body odors.

KEYWORDS

vasopressin, olfactory bulb, social discrimination, neuromodulation, neuropeptide

Introduction

Various mammalian species rely on olfaction to identify environmental stimuli, such as food, predators, or individual conspecifics. Thus, rodents sniff conspecifics at the initiation of social behaviors, allowing them to assess characteristics such as sex or familiarity. For example, male mice can discriminate urine from males and females even when they are not able to establish physical contact with them (Pankevich et al., 2004). Another example is social memory, also known as social discrimination (Engelmann et al., 2011), which is based on recognition of individual conspecifics encountered previously. This ability can be quantified experimentally as rats investigate an unknown stimulus rat longer than another with whom they recently interacted. Social memory is suggested to be highly dependent on olfaction since the olfactory bulb (OB) is essential for social discrimination (Dantzer et al., 1990).

The central actions of the neuropeptide vasopressin (VP) include the modulation of social behavior. Moreover, VP is an important enhancer of social memory (Dantzer et al., 1988). More specifically, local OB injection of a VP receptor antagonist blocks the ability to form memories of conspecifics, whereas additional local application of VP prolongs the memory for conspecifics (Dluzen et al., 1998; Tobin et al., 2010).

The OB is the very first brain region for processing and filtering olfactory signals in mammals. Neural microcircuits in the OB are known to integrate and modify signals from the olfactory epithelium before transmitting those to the olfactory cortex and other higher brain areas, which then trigger behavioral responses. Approximately 80% of all neurons in the OB are inhibitory interneurons (Shepherd et al., 2004), such as periglomerular cells (PGCs) in the glomerular layer (GL) and granule cells (GC) in the GC layer (GCL) (Nagayama et al., 2014). Interneurons form synaptic connections onto other interneurons or projection neurons, such as middle tufted cells (mTCs) and mitral cells (MCs), to inhibit them. The major portion of inhibition in the GL is suggested to function as gain control of incoming olfactory signals (e.g., Linster and Hasselmo, 1997; Cleland and Sethupathy, 2006; Cleland et al., 2007), whereas GCs organize spike timing and synchronization of projection neurons (e.g., McTavish et al., 2012; Fukunaga et al., 2014; Osinski and Kay, 2016; Egger and Kuner, 2021). Although most bulbar neurons express the classical neurotransmitter glutamate or GABA, it is known that various other substances that are released from either bulbar neurons or centrifugal projections affect neural communication in the OB as well, including neuromodulators, e.g., dopamine or acetylcholine, and neuromodulatory neuropeptides, like VP or cholecystokinin (Nagayama et al., 2014; Imamura et al., 2020; Brunert and Rothermel, 2021; Suyama et al., 2022). A source of endogenous VP that acts on social discrimination in the OB is an innate population of VP-expressing cells (VPCs) that were characterized as a subpopulation of superficial tufted cells (Tobin et al., 2010; Lukas et al., 2019). As mentioned above, VP signaling at the level of the OB is essential for the social memory of conspecifics (Tobin et al., 2010).

Several of our previous findings support the importance of VP neuromodulation in the OB during social memory establishment and thereby indicate intrabulbar VP release from VPCs. Thus, bulbar VPCs react with increased numbers of activated cells, i.e., positive for phosphorylated extracellular signal-regulated kinase, following social interaction *in vivo* and with action potential firing following olfactory nerve stimulation during acetylcholine application in *in-vitro* OB slice experiments (Suyama et al., 2021). However, it is still not clear how VP modulates olfactory processing on the cellular level to enable enhanced discrimination of very similar odor mixtures, such as conspecific body odors (Singer et al., 1997).

Tobin et al. (2010) showed that spontaneous firing rates and firing rates after odor stimulation in MCs decrease upon VP administration *in vivo*, and we showed that VP bath application decreases the amplitudes of electrical olfactory nerve (ON) stimulation-evoked excitatory postsynaptic potentials (EPSPs) in eTCs *in vitro* (Lukas et al., 2019). These initial findings suggest that VP has inhibitory effects on excitatory neurons in the OB. Since the prevalent OB VP receptors are Gq-coupled excitatory V1a receptors (V1aRs), it is unlikely that VP acts directly on excitatory neurons. Therefore, the origin of VP inhibitory effects is not yet determined. However, we have suggestions from the morphology of VPCs. We previously showed the neurite reconstruction of VPCs, including apical dendritic tufts in the GL and axons in the GCL (Lukas et al., 2019). VP-neurophysin was found in somata, dendrites, and axons, which indicates that VP could be released from dendrites, e.g., apical dendritic tufts, and axons. Biocytin-DAB reconstruction revealed that aside from apical dendritic tufts in the glomeruli, VPCs innervate densely in the GL and EPL, and in the superficial GCL, they have either numerous short but localized branches (type 1) or long-range projection along the internal plexiform layer (type 2) (Lukas et al., 2019). The observation leads to the hypothesis that VP is released in the GL and the superficial GCL binds to cells located there. In line with the hypothesis, strong signals of V1aR staining were observed in the GL (Ostrowski et al., 1994) and in the superficial part of the GCL (Tobin et al., 2010). Moreover, the discriminability of similar odors, including social discrimination, is regulated by bulbar interneurons, which in turn modulate excitatory/projection neurons (Abraham et al., 2010; Oettl et al., 2016). Thus, we hypothesized that an excitatory action of VP on inhibitory neurons in the GL or the GCL enhances the inhibition of excitatory neurons during social interactions.

As a first step to examine how VP might enhance the inhibition of excitatory neurons during odor processing, we investigated VP effects on the responses of different cell types, including both excitatory and inhibitory neurons, to ON stimulation in acute OB slices, which mimics sensory activation. Therefore, we recorded ON-evoked EPSPs and spontaneous inhibitory postsynaptic currents (IPSCs) in mTCs and MCs that project to the cortices, and ON-evoked EPSPs in PGCs and GCs. Furthermore, we performed Ca^{2+} population imaging of ON-evoked responses in the GL and the superficial GCL using two-photon microscopy.

Materials and methods

Animals

All procedures were conducted according to the guidelines for the care and use of laboratory animals by the local government of Oberpfalz and Unterfranken, and we are monitored and certified regarding animal handling and slice preparation by institutional veterinarians.

Wistar rats of either sex were purchased from Charles River Laboratories (Sulzfeld, Germany) or bred onsite in the animal facilities at the University of Regensburg. The light in the rooms was set to an automatic 12-h cycle (lights on 07:00–19:00).

Slice preparation

Eleven- to 18-day-old juvenile rats of either sex were used for *in-vitro* electrophysiology and Ca^{2+} imaging experiments. The rats were deeply anesthetized with isoflurane and quickly decapitated. Horizontal slices (300 µm) of the OB were cut in ice-cold, carbogenated ACSF (artificial cerebrospinal fluid; in mM: 125 NaCl, 26 $NaHCO_3$, 1.25 NaH_2PO_4, 20 glucose, 2.5 KCl, 1 MgCl, and 2 $CaCl_2$) using a vibratome (VT 1200, LEICA, Wetzlar, Germany) and afterward incubated in ACSF at 36°C for 45 min. Until experiments, the slices were kept at room temperature (~21°C) in ACSF.

Electrophysiology

Brain slices were placed in a recording chamber on the microscope's stage and continuously perfused with carbogenated ACSF circulated using a perfusion pump (ISM 850, Cole-Parmer, Wertheim, Germany). To perform whole-cell patch-clamp recordings, cells were visualized by infrared gradient-contrast illumination via an IR filter (Hoya, Tokyo, Japan). Glass pipettes for recordings were pulled by a pipette puller (Narishige, Tokyo, Japan) sized 4–6 MΩ and filled with intracellular solution. The intracellular solution for current-clamp recordings contained 130 K-methylsulfate, 10 HEPES, 4 $MgCl_2$, 4 Na_2ATP, 0.4 NaGTP, 10 Na phosphocreatine, and 2 ascorbate (in mM) at pH 7.2, and the intracellular solution for voltage-clamp recordings contained 110 CsCl, 10 HEPES, 4 $MgCl_2$, 10 TEA, 10 QX-314, 2.5 Na_2ATP, 0.4 NaGTP, 10 Na Phosphocreatine, and 2 ascorbate (in mM) at pH 7.2. Recordings were performed with an EPC-10 (HEKA, Lambrecht, Germany) digital oscilloscope. The series resistance ranged between 10 and 30 MΩ. The average resting membrane potentials were −60 to −70 mV in MCs and mTCs, −50 to −60 mV in PGCs, and −70 to −80 mV in GCs. Experiments were only started in cases where the patched cells had a holding current below approximately −50 pA and a stable resting membrane potential. When the resting membrane potential is shifted during the ON stimulation experiments, the holding current is adjusted to bring the membrane potential back to the initial value in order to avoid the effects of leakage and the possible direct effects of VP on the resting membrane potentials (Table 1). Experiments were performed at room temperature (~21°C).

ON stimulation was performed with a glass pipette stimulation electrode sized around 2 MΩ. Glass pipettes were filled with ACSF. The unipolar electrode was connected to an external stimulator (STG 1004, Multi-Channel Systems, Reutlingen, Germany). The stimulation strength was adjusted via the stimulator's software (MC_Stimulus, v 2.1.5), and stimulation was triggered by the amplifier software (Patchmaster, v2x73.5, HEKA). Stimulation pipettes were gently placed in the ON layer anterior to the area selected for patching using a manual manipulator (LBM-7, Scientifica, East Sussex, UK) under optical control with the microscope. The stimulation lasted for 100 µs, with a current of 20–200 µA for mTCs, 25–350 µA for MCs, 9–100 µA for PGCs, or 5–150 µA for GCs. We confirmed the identity of PGCs with *post-hoc* morphological examination. We added biocytin (5 mg/mL, Sigma-Aldrich, Darmstadt, Germany) in the intracellular solution to fill cells during recording and subsequently visualized apical dendrite arbors using enzymatic 3,3′-diaminobenzidine-based staining (Vector Laboratories, CA, USA) (Lukas et al., 2019). All patched putative PGCs had a soma sized <10 µm and no long-range laterally projecting neurite, confirming their identity as PGCs (Nagayama et al., 2014).

TABLE 1 Holding currents during experiments with olfactory nerve stimulation.

	ACSF (pA)	VP (pA)	Changes (pA)
mTCs	−40.1 ± 25.3	−42.2 ± 23.9	−1.3 ± 3.7
MCs	−34.9 ± 16.6	−37.6 ± 16.3	−2.7 ± 8.9
PGCs	−11.9 ± 15.2	−14.7 ± 15.7	−2.9 ± 4.0
GCs	−13.4 ± 17.3	−17.4 ± 18.0	−4.0 ± 5.6

mTCs, middle tufted cells; MCs, mitral cells; PGCs, periglomerular cells; GCs, granule cells.

Experimental design

In current-clamp experiments recording ON-evoked EPSPs, ON stimulation was triggered only every 30 s to prevent run-down (Lukas et al., 2019). VP was diluted in ACSF ([Arg^8]-vasopressin acetate salt, Sigma-Aldrich, Darmstadt, Germany, 1 µM) and bath-applied via the perfusing system after a baseline recording of 5 min. Traces in the VP condition were recorded no earlier than 5 min after the onset of administration. Traces were averaged over five stimulations, and two such averaged traces, each in the ACSF condition and in the VP condition, were analyzed. Averaged amplitudes within conditions were normalized to the ACSF condition (100%). The data were analyzed with Origin 2020 (Origin Lab Corporation, Northampton, MA, USA).

In voltage-clamp experiments, spontaneous IPSCs were recorded at 0 mV for 10 min during each condition. VP (1 µM) was bath-applied via the perfusion system, and the VP condition was recorded 5 min after the onset of administration for 5 min. The frequencies and amplitudes of IPSCs were normalized to the ACSF condition (100%). The data were analyzed with the Peak Analyzer in Origin 2020.

Population Ca^{2+} imaging

For population Ca^{2+} imaging, the AM-dye Cal-520 (1 µM, AAT Bioquest, CA, USA) and Alexa 594 (50 µM, Invitrogen) were loaded into the superficial GCL or the GL via a glass pipette sized around 2 MΩ. Loading pipettes were guided by light microscopy and the Alexa 594 fluorescence. The Ca^{2+} dye was loaded for 15 s using the Picospritzer III device (Parker Hannifin, NH, USA), followed by 20 min incubation to allow the Ca^{2+} dye to be taken up by cells. The fluorescence was imaged at a wavelength of 850 nm in raster-scan mode using a two-photon resonant scanner (frame rate of 31.5 Hz). Femto-2D microscope (Femtonics) was equipped with a Mai Tai wideband, mode-locked Ti:Sapphire laser (Spectra-Physics, CA, USA) and a 20× Zeiss water immersion objective (Carl Zeiss, Oberkochen, Germany). The microscope was controlled by MESc v3.3.4290 software (Femtonics). ON stimulation (400 µA, 100 µs) was applied three times for each condition: control (ACSF) and VP (1 µM). VP was bath-applied via the perfusion system, and the VP condition was recorded 10 min after the onset of administration.

The raw data of the experiments were imported to Fiji[1] and ΔF/F in the somata of GCs, juxtaglomerular cells (JGCs, decided by the small cell bodies), and the glomeruli were extracted using the ROI selection tool. The resulting traces from the three stimulations per condition were averaged. ΔF/F amplitudes and integral (from the onset of the signal until the signal is back to the baseline or the end of the session) were analyzed with Origin 2020. ΔF/F in the VP condition was corrected according to the ratio of the basal fluorescence (F0) in the VP condition to that in the ACSF condition. Corrected ΔF/F

1 ImageJ, downloaded from: https://imagej.net/Fiji/Downloads.

(VP) = ΔF/F (VP) × F0 (VP) / F0 (ACSF). Averaged amplitudes and integral within conditions were normalized to the ACSF condition (100%).

Ca^{2+} imaging experiments were performed at room temperature (~21°C).

Statistics

Statistics were performed with SPSS (version 26, IBM, Armonk, NY, USA). All statistical analysis performed was two-sided, and significance was accepted at $p < 0.05$. All data in the text are shown with average ± standard deviation.

Results

VP reduced ON-mediated excitation and increased spontaneous inhibition in mTCs but not in MCs

We performed patch-clamp recordings in either current-clamp or voltage-clamp configuration in mTCs and MCs in acute OB slices (Figure 1A). Electrical ON stimulation reliably evoked EPSPs in mTCs and MCs. We then compared EPSP amplitudes in the presence of VP (1 µM in ACSF) to the control condition (ACSF). In mTCs, VP reduced the amplitudes of ON-evoked EPSPs to 60.4 ± 20.5% of control ($p = 0.012$, $z = -2.521$, related samples Wilcoxon test, $n = 8$ from six rats; Figures 1B,C). The amplitudes of ON-evoked EPSPs without VP application were stable over time compared to the VP condition (95.0 ± 4.6% of control, 10 min after the start of the measurement, $n = 5$ from four rats, $p = 0.004$, $t(11) = 3.657$, t-test vs. VP). Therefore, we concluded that the reduction is due to VP application but not desensitization of bulbar circuits to ON stimulation. In another set of experiments using voltage-clamp recordings, VP increased the frequencies of spontaneous IPSCs to 123.3 ± 23.6% of control ($p = 0.012$, $z = 2.521$, related samples Wilcoxon test, $n = 8$ from four rats; Figures 1D,E). However, the amplitudes of spontaneous IPSCs were not changed (106.9 ± 24.3%, $p = 0.263$, $z = 1.120$, related samples Wilcoxon test, $n = 8$ from four rats; Figure 1F), indicating a predominantly presynaptic effect. Furthermore, in all experiments ($n = 8$ from four rats), spontaneous IPSCs were abolished following bath application of bicuculline (a GABA receptor antagonist, 50 µM), confirming the GABAergic origin of these signals (data not shown). Therefore, the data imply that VP enhances both ON-evoked and tonic inhibitory modulation of mTCs. Surprisingly, we did not observe any of those VP inhibitory effects in MCs, even though broad distributions in evoked EPSP amplitudes and IPSC frequencies in the VP condition were observed [ON-evoked EPSPs: 99.4 ± 20.2% of control, $p = 0.929$, $z = -0.089$,

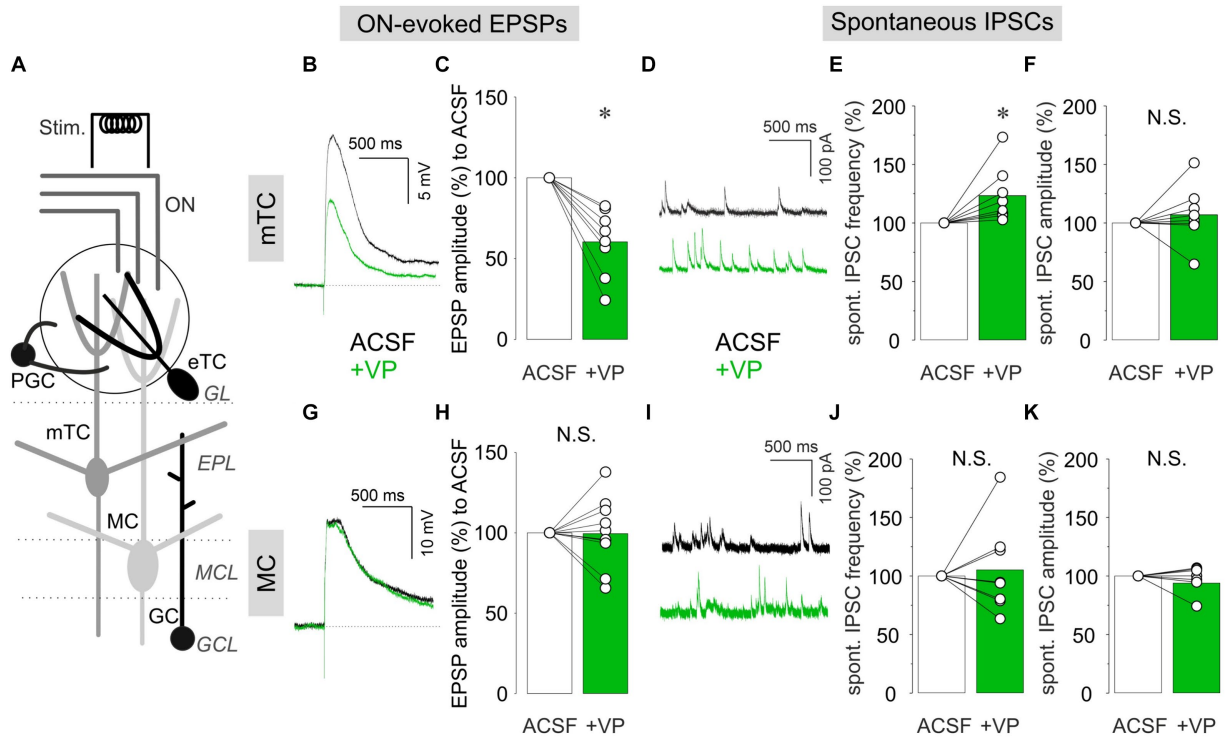

FIGURE 1
Patch-clamp recordings from mTCs and MCs. **(A)** The schematic image of the OB slice. ON, olfactory nerve; GL, glomerular layer; EPL, external plexiform layer; MCL, mitral cell layer; GCL, granule cell layer; Stim., electrical ON stimulation; PGC, periglomerular cell; eTC, external tufted cell; mTC, middle tufted cell; MC, mitral cell; GC, granule cell. Representative current-clamp traces of ON-evoked EPSPs and cumulative data of ON-evoked EPSP amplitudes in % to control in mTCs **(B,C)** and MCs **(G,H)**. Representative voltage-clamp traces of spontaneous IPSCs and cumulative data of spontaneous IPSC frequencies and amplitudes in % to control in mTCs **(D–F)** and MCs **(I–K)**. The bar graphs show average values. Individual data points are shown as open circles, and points from the same cell are connected by a line. *$p < 0.05$; N.S., non-significant. Black traces: ACSF (control); Green traces: VP.

related samples Wilcoxon test, $n = 11$ from nine rats (Figures 1G,H); frequencies of spontaneous IPSCs: 105.3 ± 38.2% of control, $p = 0.889$, $z = 0.140$, related samples Wilcoxon test, $n = 8$ from six rats (Figures 1I,J); amplitudes of spontaneous IPSCs: 97.2 ± 10.6% of control, $p = 0.779$, $z = -0.280$, related samples Wilcoxon test, $n = 8$ from six rats (Figures 1I,K)]. This lack of consistent inhibitory effects in MCs was somewhat unexpected, as Tobin et al. (2010) showed *in vivo* that VP reduces spontaneous and odor-evoked spiking rates in MCs.

VP did not increase evoked EPSPs in inhibitory neurons

Where does the inhibition of excitatory projection neurons, e.g., eTCs or mTCs, originate from? There are two main populations of inhibitory interneurons in the OB. One is in the glomerular layer (GL), where synapses between the ON and bulbar neurons reside within the glomerular neuropil. Thus, the first modulation of olfactory inputs takes place in this layer. There are many cell types of inhibitory neurons in the GL, and the most numerous are PGCs (Nagayama et al., 2014). We performed patch-clamp recordings in PGCs regardless of subtypes, as we were not able to differentiate them in our experimental setup. ON stimulation-evoked EPSPs in PGCs. We observed mixed effects of VP (1 μM) on the amplitudes of evoked EPSPs, including increase, decrease, or no changes (Figure 2A). Consequently, there was no overall significant difference between VP application compared to the control condition (85.4 ± 26.1% of control, $p = 0.131$, $z = -1.511$, paired Wilcoxon test, $n = 11$ from nine rats; Figure 2B). We further categorized PGCs into either Type A or Type C according to their firing patterns, as described by Tavakoli et al. (2018). In addition, we examined if hyperpolarizing currents evoked sags due to hyperpolarization-induced depolarization. Moreover, we visualized patched putative PGCs by filling cells with biocytin (see methods) to investigate their morphology. However, we could not find any correlation between these electrophysiological or morphological characteristics and the different directions of VP effects (data not shown).

We next examined the second main population of inhibitory interneurons in the OB, the GCs (Nagayama et al., 2014). Unlike PGCs, VP consistently decreased the amplitudes of ON-evoked EPSPs in GCs to 85.0 ± 11.7% of control ($p = 0.012$, $z = -2.521$, related samples Wilcoxon test, $n = 8$ from eight rats; Figures 2C,D). Thus, ON-evoked EPSPs were not increased upon VP administration in both inhibitory interneuron populations, arguing against an increased excitation of interneurons via the sensory afferents as a mechanism for the inhibitory action of VP on eTCs and mTCs.

VP increased evoked Ca^{2+} influx in inhibitory neurons

While VP did not increase the subthreshold excitability of inhibitory neurons, we next wondered whether suprathreshold activation might be enhanced. Therefore, we performed two-photon population Ca^{2+} imaging to examine VP effects on Ca^{2+} influx in inhibitory interneurons with strong ON stimulation, which is likely to evoke action potentials in stimulated cells from our experience (400 μA, up to 100 μA, or 150 μA for EPSP experiments in PGCs or GCs, respectively). We injected the AM-dye Cal-520 into the GL, followed by two-photon imaging with a resonant scanner. After JGCs took up the dye into their somata, we stimulated the ON and measured ΔF/F in the JGC somata as well as in the neuropil in the glomeruli (Figures 3A,B; Egger et al., 2003). F0 in JGCs increased in the VP condition to 125 ± 29.3% of control ($p < 0.001$, $z = 8.882$, related samples Wilcoxon test; Figure 3C). While there were mixed effects, on average VP significantly increased the amplitudes and the integral of ON-evoked ΔF/F changes to 156 ± 101% and 143 ± 106% of control, respectively [Amplitudes: $p < 0.001$, $z = 6.376$, related samples Wilcoxon test; Integral: $p < 0.001$, $z = 3.775$, related samples Wilcoxon test, $n = 166$ from five rats (Figures 3B,C)]. F0 in the glomeruli increased in the VP condition to 110 ± 14.8% of control ($p = 0.041$, $z = 2.040$, related samples Wilcoxon test; Figure 3D). The amplitudes and the

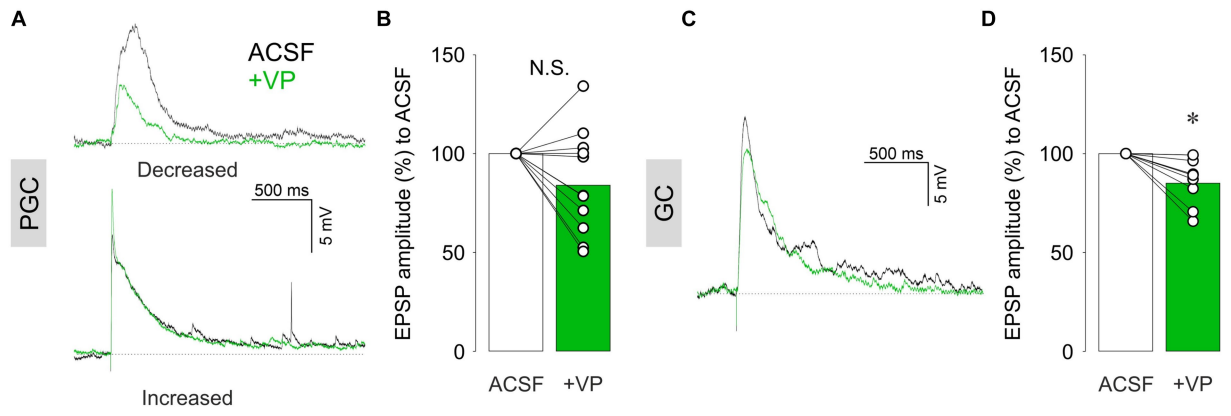

FIGURE 2
Representative current-clamp traces of ON-evoked EPSPs and cumulative data of ON-evoked EPSP amplitudes in % to control in PGCs **(A,B)** and GCs **(C,D)**. The bar graphs show average values. Individual data points are shown as open circles, and points from the same cell are connected by a line. *$p < 0.05$; N.S., non-significant. Black traces: ACSF (control); Green traces: VP.

10.3389/fncir.2024.1448592

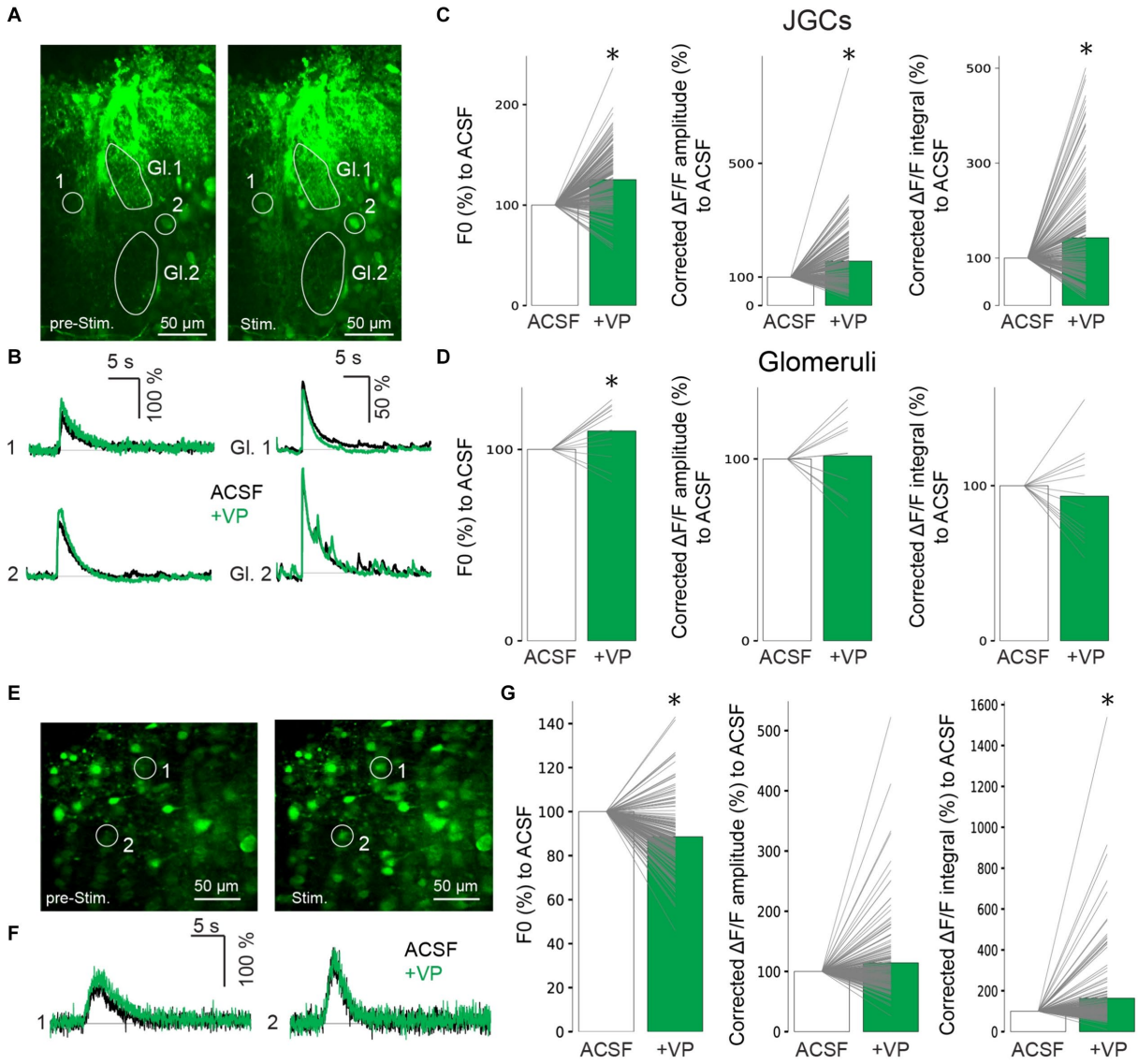

FIGURE 3
Representative images of Ca^{2+} imaging before ON stimulation (left) and after ON stimulation (right) in the GL **(A)**. Gl., glomerulus. Representative traces of Ca^{2+} imaging from corresponding JGCs (left) and from corresponding glomeruli (right) in A **(B)**. Cumulative data of F0 (left) and amplitudes (middle) and integral (right) of ΔF/F in JGCs **(C)** and glomeruli **(D)**. Bar graphs show average values. Individual data points from the same cell are connected by a line. *$p < 0.05$. Black traces: ACSF (control); Green traces: VP. Representative images of Ca^{2+} imaging before ON stimulation (left) and after ON stimulation (right) in the GCL **(E)**. Representative traces of Ca^{2+} imaging from the corresponding GCs are shown in E **(F)**. Cumulative data of F0 (left) and amplitudes (middle) and integral (right) of ΔF/F in GCs **(G)**. The bar graphs show average values. Individual data points from the same cell are connected by a line. *$p < 0.05$. Black traces: ACSF (control); Green traces: VP.

integral of ON-evoked ΔF/F in the glomeruli were similar to control, 102 ± 21.6% and 93.3 ± 30.3% of control, respectively [Amplitudes: $p = 0.754$, $z = 0.314$, related samples Wilcoxon test; Integral: $p = 0.388$, $z = -0.863$, related samples Wilcoxon test, $n = 12$ from five rats (Figures 3B,D)].

We also performed dye injections in the superficial GCL and measured changes in intracellular Ca^{2+} levels in the GC somata (Figures 3E,F). F0 decreased in the VP condition to 88.6 ± 15.3% of the control ($p < 0.001$, $z = -7.973$, related samples Wilcoxon test; Figure 3G). In these experiments, again, there were mixed effects, but on average, VP significantly increased the integral but not the amplitudes of ON-evoked ΔF/F changes to 164 ± 181% and 114 ± 63% of control, respectively [Integral: $p < 0.001$, $z = 3.832$, related samples Wilcoxon test; Amplitudes: $p = 0.558$, $z = 0.587$, related samples Wilcoxon test, $n = 165$ from six rats (Figures 3F,G)].

Therefore, we suggest that VP enhances evoked Ca^{2+} influx in those inhibitory interneurons (Table 2).

Discussion

Origin of VP inhibitory effects in the OB

V1aRs that are predominantly expressed in the olfactory bulb are $G\alpha_{q/11}$-coupled receptors and thus act in an excitatory manner (Birnbaumer, 2002). As mentioned in the introduction, V1aRs are

TABLE 2 Summary of results regarding ON-evoked responses in different neuron types.

		Subthreshold activation (E/IPSPs) Weak ON stimulation	Suprathreshold activation (Ca^{2+} influx) Strong ON stimulation
Excitatory neurons	eTCs (Lukas et al., 2019)	↓ (ON-evoked EPSPs)	–
	mTCs	↓ (ON-evoked EPSPs)↑ (spontaneous IPSPs)	–
	MCs	N.S. (ON-evoked EPSPs, spontaneous IPSPs)	–
Inhibitory neurons	JGCs/PGCs	N.S. (ON-evoked EPSPs)	↑ (amplitude, integral)
	GCs	↓ (ON-evoked EPSPs)	N.S. (amplitude)/ ↑ (integral)

eTCs, external tufted cells; mTCs, middle tufted cells; MCs, mitral cells; JGCs, juxtaglomerular cells; PGCs, periglomerular cells; GCs, granule cells; N.S., non-significant.

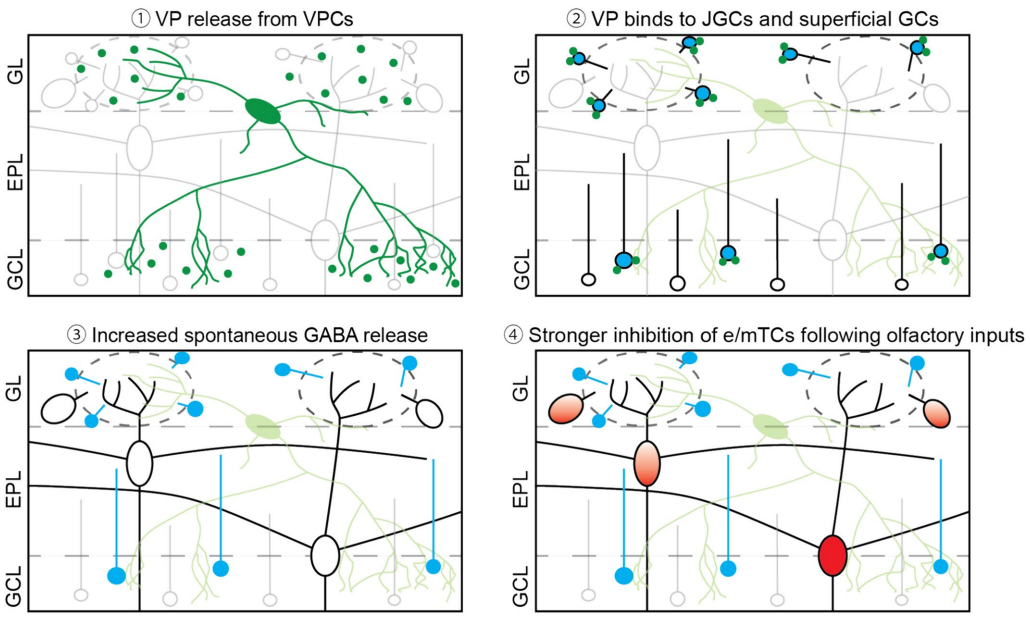

FIGURE 4
Scheme of the overview. (1) Once VPCs are activated, VP is released from their dendrites and axons in both the GL and the superficial GCL. (2) Released VP binds to VP receptors, which are expressed in the GL and the superficial GCL, likely on JGCs and GCs. (3) Through VP receptor activation, spontaneous GABA release occurs more frequently, leading to more spontaneous inhibitory inputs onto mTCs. (4) Following suprathreshold olfactory inputs, VP-bound interneurons are activated stronger and then inhibit e/mTCs and MCs (Tobin et al., 2010).

expressed in the GL and the superficial part of the GCL (Ostrowski et al., 1994; Tobin et al., 2010). In addition, VPCs innervate densely those two layers in the OB (Figure 4; Lukas et al., 2019). This distribution of V1aRs and VPC's innervation fits our data, showing that VP increased the ON-evoked Ca^{2+} signal in JGCs and GCs in those layers. Moreover, VP increases the inhibition of eTCs (Lukas et al., 2019) and mTCs (Figure 1). A similar VP-mediated increase of inhibition has been shown in other brain regions. For example, VP increases the frequency of spontaneous IPSP/Cs in magnocellular paraventricular nucleus neurons (Hermes et al., 2000), as well as spontaneous spikes in hippocampal GABAergic neurons, which results in an increase in the number of spontaneous IPSCs in pyramidal neurons (Ramanathan et al., 2012). Ramanathan et al. (2012) suggested that increased hippocampal GABAergic inhibition of pyramidal cells may result in organized inhibition to establish fine-tuning of excitation and rhythmic synchronized activity of pyramidal neurons that are important for memory consolidation. Since the function of bulbar inhibitory networks is suggested to tune excitation and modulate oscillatory activity as well, VP effects on bulbar inhibitory neurons may help organize excitatory neuron activity.

In current-clamp experiments, we did not observe significant changes in the holding current to keep the basal membrane potentials the same as the initial values between control and the VP condition, and the changes are not different between cell types (Table 1; mTCs: $p = 0.348$, $t(7) = 1.006$, paired t-test; MCs: $p = 0.341$, $t(10) = 1.000$, paired t-test; PGCs: $p = 0.061$, $t(10) = 2.108$, paired t-test; GCs: $p = 0.082$, $t(7) = 2.028$, paired t-test; Between cell types: $p = 0.285$, $H = 3.788$, $df = 3$, Kruskal–Wallis test). Even though holding currents tend to be more negative in the VP condition, implying depolarization, changes are not statistically significant, and we cannot differentiate potential VP effects and the increase of leakage currents over time. F0 in the Ca^{2+} population imaging showed different results in the GL and the GCL. F0 in JGCs and glomeruli significantly increased (Figures 3C,D), and F0 in GCs significantly decreased (Figure 3G) in the VP condition. One can assume that VP increases the basal Ca^{2+} concentration in JGCs and

decreases it in GCs. However, the dye has been shown to suffer from F0 increases over time (Tada et al., 2014). In addition, photobleaching should be considered. As a result, we cannot definitely conclude what causes the F0 changes from our experiments. Therefore, further experiments focusing on the VP effects on the resting membrane potentials or basal Ca^{2+} concentrations in OB neurons would be beneficial to better understand the direct effects of VP. Previous studies on the VP effects on the hippocampus (Urban and Killian, 1990) and the lateral septum (Van Den Hooff and Urban, 1990) showed that only a subset of neurons depolarized and/or fired upon VP application. However, even neurons that did not get directly excited by VP showed synaptic modulation by VP. Thus, even if VP does not change their resting membrane potentials, other mechanisms, e.g., intracellular cascades involving ER Ca^{2+} or DAG (Birnbaumer, 2002), would contribute to changing the response to the inputs, such as greater Ca^{2+} influx.

Functional implication of the VP effects: different results with weak or strong ON inputs

Functional differences between PGCs (inhibition in the GL) and GCs have been discussed extensively elsewhere (see review, Devore and Linster, 2012, D'Souza and Vijayaraghavan, 2014). Briefly, inhibition in the GL tunes activation patterns of projection neurons, such as contrast enhancement or concentration invariance (e.g., Linster and Hasselmo, 1997; Cleland and Sethupathy, 2006; Cleland et al., 2007). For instance, acetylcholine (ACh), which is known to activate GL interneurons (Devore and Linster, 2012), enhances the contrast of projection neural representation responding to very similar odors. Thus, neostigmine (an acetylcholinesterase inhibitor) administration in the OB increases differences in the number of MC spikes between responses to ethers differing by single carbon chain in *in-vivo* electrophysiology. For example, an MC responds strongest to E2 (ethyl acetate) and second strongest to E3 (ethyl propionate), differing by only one carbon chain, but the responses are not significantly different from each other. In the presence of neostigmine, the MC responds less strongly to or gets more inhibited by E3 than control. Therefore, responses of the MC to E2 and E3 are discriminable (Chaudhury et al., 2009). Moreover, electrical stimulation of the horizontal limb of the diagonal band of Broca (HDB), the center of cholinergic top-down projections, decreases glomerular M/TC-tuft activity following odor presentation with high concentration, whereas increases glomerular activity following low-concentration odor presentation in *in-vivo* Ca^{2+} imaging, indicating responses are less varied to different concentrations of the same odor (Bendahmane et al., 2016). These authors suggested that the less variation of responses to different odor concentrations makes neural representation reflect more purely the identity of odors. In our hands, VP increased the amplitudes of ON-evoked Ca^{2+} influx into JGCs in population imaging. If VP effects and ACh effects on the GL interneurons are similar, VP might prevent excitatory neurons from firing when they are weakly activated. Therefore, we observed inhibitory VP effects on the amplitudes of subthreshold-evoked EPSPs in eTCs (Lukas et al., 2019) and mTCs (Figure 1). The lack of inhibitory effects on MCs is discussed below.

GCs are responsible for the organization of spike timing and synchronization of projection neurons that further refine contrast and representations of odors (e.g., McTavish et al., 2012; Osinski and Kay, 2016). Computational analysis showed that the level of GC excitability might tune oscillatory frequency in MCs; thus, with low excitability of GCs, MCs fire in the gamma range, however high excitability allows MCs to fire in beta oscillation (Osinski and Kay, 2016). Oettl et al. (2016) showed the modulation of GCs via the oxytocin system in the anterior olfactory nucleus (AON). An oxytocin receptor agonist increases the frequency of spontaneous EPSCs in GCs from AON excitatory neurons, resulting in increased spontaneous IPSCs in MCs. In *in-vivo* electrophysiological recordings in M/TCs, an oxytocin receptor agonist applied in the AON lowers basal spiking rates and increases odor-evoked spiking rates, thus improving the signal-to-noise ratio. Conditional oxytocin receptor knockout in the AON impairs social memory, showing that the enhanced signal-to-noise ratio in M/TCs by activation of GCs is important for discrimination of conspecific body odors (Oettl et al., 2016).

Interestingly, the results of ON-evoked EPSPs and ON-evoked Ca^{2+} influx in PGCs (or JGCs) and GCs contradict each other (Figures 2, 3). This discrepancy may be explained by the fact that what we were observing during recording EPSPs and imaging Ca^{2+} influx is different. During slice experiments, we performed subthreshold activation, whereas, during Ca^{2+} imaging, we performed suprathreshold activation by ON stimulation. Possibly, VP can enhance Ca^{2+} entry selectively for suprathreshold activation, which is probably not related to the initial depolarization but to later phases of the signal which involve contributions from NMDARs. V1aRs and NMDARs are present at GC somata (Personal communication with M. Sassoe-Pognetto; Stroh et al., 2012). In the rat ventral hippocampus, VP excites neurons, and the VP effects are blocked by both V1aR and NMDAR antagonists, indicating VP effects via modulation of NMDARs. Moreover, VP enhances glutamate-evoked spiking (Urban and Killian, 1990). In contrast, EPSPs are subthreshold activation that are highly dependent on the inputs of the cells. We observed the inhibitory VP effects on excitatory neurons (Figure 1; Tobin et al., 2010, Lukas et al., 2019). The results indicate that the inputs of inhibitory interneurons, e.g., glutamate released from excitatory neurons, are less in the presence of VP. Hence, smaller amplitudes of evoked EPSPs in GCs in the VP condition that we observed. Mixed results in PGCs might be due to the differences in connectivity, either directly connected with the ON or with eTCs (Shao et al., 2009), e.g., the ON-driven population is resistant and the eTC-driven population is susceptible to the VP administration because eTCs are susceptible. Although we did not observe subpopulations that can be divided by the VP effects on EPSP amplitudes, morphology, or firing pattern, it is worth examining further characteristics, such as molecular markers. We have not performed experiments on interneurons in the EPL (Nagayama et al., 2014). Since VPC's neurites are found in the EPL, it would be informative to investigate VP effects on them as well.

Our data showed that VP reduced the amplitudes of ON-evoked EPSPs in eTCs (Lukas et al., 2019) and mTCs. These data indicate that eTCs and mTCs need stronger ON inputs to fire under the VP condition. The suppression of those neurons could result in contrast enhancement of the neural representation in the OB (Chaudhury et al., 2009). The glomerular GABAergic inhibition includes $GABA_A$ receptor- and $GABA_B$ receptor-mediated pathways. For instance, cholecystokinin, which is also expressed in a subpopulation of superficial tufted cells, acts on SACs to inhibit presynaptically the ON via $GABA_B$ receptors, resulting in smaller ON-evoked EPSCs in eTCs (Liu and Liu, 2018). Therefore, a similar mechanism is conceivable for

VP modulation, and further examination of the involvement of SACs or $GABA_B$ receptors would give us more insights into the VP-mediated inhibition of eTCs and mTCs. Interestingly, unlike for mTCs or eTCs, VP did not reduce the amplitudes of evoked EPSPs or increase frequencies of spontaneous IPSCs in MCs. This variance in our data between mTCs and MCs could be due to the difference in input sources of the two cell types. MCs receive indirect excitatory inputs from eTCs (De Saint Jan et al., 2009; Najac et al., 2011), and MCs are less sensitive to odor inputs than e/mTCs (Igarashi et al., 2012). If the ON-evoked EPSPs in MCs are consequences of the firing of eTCs, the ON stimulation intensity in MC experiments may be strong for eTCs, so that also during VP application, APs are still evoked in eTCs. Thus, during VP application, the same net amount of excitation is transmitted to MCs as without VP. Tobin et al. (2010) showed that odor-evoked MC firing decreased upon VP administration, although we did not observe reduced amplitudes of ON-evoked EPSPs in MCs in our experiments (Figure 1). In their *in-vivo* experiments, Tobin et al. (2010) presented odors that were able to fire MCs. We purposefully stimulated the ON electrically in *in-vitro* slices to evoke EPSPs in MCs. Thus, we suggest that the discrepancy between the results from Tobin et al. (2010) and ours might be due to differences in subthreshold and suprathreshold activation of MCs in the different experimental setups. The main inputs of GCs are dendrodendritic glutamatergic signals from TCs or MCs. If the somata of MCs do not show active conduction like in our slice experiments, it is unlikely that their lateral dendrites release glutamate to excite GCs. As a result, inhibition of MC firing via dendrodendritically induced GABA release from GCs cannot be triggered or modulated by VP. However, during strong ON stimulation, like odor stimulation, MCs fire and excite GCs. If the excitation is strong enough, VP could enhance the GC activity as also shown in our Ca^{2+} imaging experiments using suprathreshold ON stimulation (Figure 3). Under these conditions, VP-modulated enhanced activation of GCs might be responsible for an increased dendrodenritic GABAergic suppression of MC firing as shown in the *in-vivo* experiments of Tobin et al. (2010). However, to finally confirm this hypothesis, further Ca^{2+} imaging or spike analysis experiments using strong ON stimulation would be needed. Since Tobin et al. (2010) reported that V1aRs are expressed in MCs as well, we cannot exclude that VP directly excites MCs, even though we could not see excitatory effects in our experiments. In CA1, VP increases not only the number of spontaneous IPSCs but also the number of spontaneous spikes under the conditions of glutamatergic and GABAergic receptor antagonists in pyramidal neurons (Ramanathan et al., 2012). Therefore, the non-synaptic excitability of projection neurons would be intriguing to examine, as mentioned above. Sun et al. (2021) showed interesting effects of oxytocin, which also modulates social discrimination at the level of the OB (Dluzen et al., 1998; Sun et al., 2021). The authors demonstrated that oxytocin directly reduces the excitability of MCs via the Gq protein pathway, which, in turn, results in less activation of GCs responding to odor presentation. As a direct mechanism like that one is also conceivable for VP via V1aR on MCs, these results further encourage the examination of direct VP effects on MCs.

In addition to VP and oxytocin, various other neuropeptides are involved in the modulation of OB neuron activity (Stark, 2024). For instance, Decoster et al. (2024) recently showed that GnRH (gonadotropin-releasing hormone)-expressing neurons in male mice are activated upon the presentation of estrus female urine, and silencing of GnRH neurons impairs preference toward estrus female urine over male urine in male mice. Although it is not clear yet how other neuropeptides modulate neural activity in the OB in social contexts, it is worth paying attention to other neuropeptidergic systems. In addition, there might be synergic effects of different neuropeptides, especially ones that are known to have similar behavioral effects, such as VP and oxytocin (Dluzen et al., 1998; Tobin et al., 2010; Sun et al., 2021; Suyama et al., 2021).

Possible consequences of VP-mediated OB modulation

We previously suggested that social discrimination is a variation of perceptual learning because of the association with ACh and the close similarity of stimuli, i.e., conspecific body odors, that rats discriminate (Suyama et al., 2021). Perceptual learning is possible because a subject pays attention to a stimulus during exposures, and sensory acuity against the stimulus is enhanced due to a finer neural representation. As mentioned above, ACh, an important substance for perceptual learning, increases differences in the number of MC spikes reacted to odors differing by a single carbon (Chaudhury et al., 2009). This change in neural representation results in behavioral outputs like habituation. Rats lose their motivation to investigate odor if rats perceive it as the same one as they previously investigated, i.e., habituation. In controls, rats show habituation to an odor differing by a single carbon from a previously exposed odor, suggesting that rats cannot distinguish odors differing by one carbon. However, injection of neostigmine into the OB enables rats to discriminate those odors (Chaudhury et al., 2009). Therefore, neuromodulation of projection neuron activity seems to be important for sensory perception, hence discrimination as the behavioral output of this enhanced sensory perception. We demonstrated that VP modulation may result in less mTCs firing via GL contrast enhancement. Furthermore, VP inhibits the firing rates of MCs (Tobin et al., 2010), which can result in improved neural representation (Linster and Hasselmo, 1997). Although Tobin et al. (2010) did not record the firing rates of mTCs, it is plausible that this is the same for all projection neurons. Thus, in the VP condition, M/TCs may transmit more precise information to higher brain regions, like during the modulatory action of ACh (Chaudhury et al., 2009). Taken together, we hypothesize that VP inhibits projection neurons differently to reduce sensitivity and improve representation in the olfactory cortex.

Data availability statement

The raw data supporting the conclusions of this article will be made available by the authors, without undue reservation.

Ethics statement

Ethical approval was not required for the study involving animals in accordance with the local legislation and institutional requirements because according to the German Animal Ethics Legislature, killing animals exclusively for the purposes of using their organs or tissues is not considered as an animal experiment (Tierschutzgesetz, Section 4,

Paragraph 3). We are monitored and certified regarding animal handling and slice preparation by institutional veterinarians.

Author contributions

HS: Funding acquisition, Writing – review & editing, Writing – original draft, Visualization, Supervision, Methodology, Investigation, Formal analysis, Data curation, Conceptualization. GB: Writing – review & editing, Data curation. ML: Writing – review & editing, Writing – original draft, Visualization, Supervision, Project administration, Methodology, Investigation, Funding acquisition, Formal analysis, Data curation, Conceptualization.

Funding

The author(s) declare that financial support was received for the research, authorship, and/or publication of this article. This research was supported by the German Research Foundation (DFG LU2164/1-1), the Boehringer Ingelheim Fonds (travel grant), and the University of Regensburg (RU5424).

Acknowledgments

We would like to thank Anne Pietryga-Krieger for experimental support, Christoph Schmid and Atefeh Akbari for help with experimentation, and Veronica Egger for experimental equipment such as electrophysiology rigs and Ca^{2+} imaging setups and advice.

Conflict of interest

The authors declare that the research was conducted in the absence of any commercial or financial relationships that could be construed as a potential conflict of interest.

Publisher's note

References

Abraham, N. M., Egger, V., Shimshek, D. R., Renden, R., Fukunaga, I., Sprengel, R., et al. (2010). Synaptic inhibition in the olfactory bulb accelerates odor discrimination in mice. *Neuron* 65, 399–411. doi: 10.1016/j.neuron.2010.01.009

Bendahmane, M., Ogg, M. C., Ennis, M., and Fletcher, M. L. (2016). Increased olfactory bulb acetylcholine bi-directionally modulates glomerular odor sensitivity. *Sci. Rep.* 6:25808. doi: 10.1038/srep25808

Birnbaumer, M. (2002). "58 - vasopressin receptors" in Hormones, brain and behavior. eds. D. W. Pfaff, A. P. Arnold, S. E. Fahrbach, A. M. Etgen and R. T. Rubin (San Diego: Academic Press).

Brunert, D., and Rothermel, M. (2021). Extrinsic neuromodulation in the rodent olfactory bulb. *Cell Tissue Res.* 383, 507–524. doi: 10.1007/s00441-020-03365-9

Chaudhury, D., Escanilla, O., and Linster, C. (2009). Bulbar acetylcholine enhances neural and perceptual odor discrimination. *J. Neurosci.* 29, 52–60. doi: 10.1523/JNEUROSCI.4036-08.2009

Cleland, T. A., Johnson, B. A., Leon, M., and Linster, C. (2007). Relational representation in the olfactory system. *Proc. Natl. Acad. Sci.* 104, 1953–1958. doi: 10.1073/pnas.0608564104

Cleland, T. A., and Sethupathy, P. (2006). Non-topographical contrast enhancement in the olfactory bulb. *BMC Neurosci.* 7:7. doi: 10.1186/1471-2202-7-7

D'souza, R. D., and Vijayaraghavan, S. (2014). Paying attention to smell: cholinergic signaling in the olfactory bulb. *Front. Synaptic Neurosci.* 6:21. doi: 10.3389/fnsyn.2014.00021

Dantzer, R., Koob, G. F., Bluthe, R. M., and Lemoal, M. (1988). Septal vasopressin modulates social memory in male-rats. *Brain Res.* 457, 143–147. doi: 10.1016/0006-8993(88)90066-2

Dantzer, R., Tazi, A., and Bluthe, R. M. (1990). Cerebral lateralization of olfactory-mediated affective processes in rats. *Behav. Brain Res.* 40, 53–60. doi: 10.1016/0166-4328(90)90042-D

De Saint Jan, D., Hirnet, D., Westbrook, G. L., and Charpak, S. (2009). External tufted cells drive the output of olfactory bulb glomeruli. *J. Neurosci.* 29, 2043–2052. doi: 10.1523/JNEUROSCI.5317-08.2009

Decoster, L., Trova, S., Zucca, S., Bulk, J., Gouveia, A., Ternier, G., et al. (2024). A Gnrh neuronal population in the olfactory bulb translates socially relevant odors into reproductive behavior in male mice. *Nature Neurosci.* doi: 10.1038/s41593-024-01724-1

Devore, S., and Linster, C. (2012). Noradrenergic and cholinergic modulation of olfactory bulb sensory processing. *Front. Behav. Neurosci.* 6:52. doi: 10.3389/fnbeh.2012.00052

Dluzen, D. E., Muraoka, S., Engelmann, M., and Landgraf, R. (1998). The effects of infusion of arginine vasopressin, oxytocin, or their antagonists into the olfactory bulb upon social recognition responses in male rats. *Peptides* 19, 999–1005. doi: 10.1016/S0196-9781(98)00047-3

Egger, V., and Kuner, T. (2021). Olfactory bulb granule cells: specialized to link coactive glomerular columns for percept generation and discrimination of odors. *Cell Tissue Res.* 383, 495–506. doi: 10.1007/s00441-020-03402-7

Egger, V., Svoboda, K., and Mainen, Z. F. (2003). Mechanisms of lateral inhibition in the olfactory bulb: efficiency and modulation of spike-evoked calcium influx into granule cells. *J. Neurosci.* 23, 7551–7558. doi: 10.1523/JNEUROSCI.23-20-07551.2003

Engelmann, M., Hadicke, J., and Noack, J. (2011). Testing declarative memory in laboratory rats and mice using the nonconditioned social discrimination procedure. *Nat. Protoc.* 6, 1152–1162. doi: 10.1038/nprot.2011.353

Fukunaga, I., Herb, J. T., Kollo, M., Boyden, E. S., and Schaefer, A. T. (2014). Independent control of gamma and theta activity by distinct interneuron networks in the olfactory bulb. *Nat. Neurosci.* 17, 1208–1216. doi: 10.1038/nn.3760

Hermes, M. L. H. J., Ruijter, J. M., Klop, A., Buijs, R. M., and Renaud, L. P. (2000). Vasopressin increases Gabaergic inhibition of rat hypothalamic paraventricular nucleus neurons *in vitro*. *J. Neurophysiol.* 83, 705–711. doi: 10.1152/jn.2000.83.2.705

Igarashi, K. M., Ieki, N., An, M., Yamaguchi, Y., Nagayama, S., Kobayakawa, K., et al. (2012). Parallel mitral and tufted cell pathways route distinct odor information to different targets in the olfactory cortex. *J. Neurosci.* 32, 7970–7985. doi: 10.1523/JNEUROSCI.0154-12.2012

Imamura, F., Ito, A., and Lafever, B. J. (2020). Subpopulations of projection neurons in the olfactory bulb. *Front. Neural Circuits* 14. doi: 10.3389/fncir.2020.561822

Linster, C., and Hasselmo, M. (1997). Modulation of inhibition in a model of olfactory bulb reduces overlap in the neural representation of olfactory stimuli. *Behav. Brain Res.* 84, 117–127. doi: 10.1016/S0166-4328(97)83331-1

Liu, X., and Liu, S. (2018). Cholecystokinin selectively activates short axon cells to enhance inhibition of olfactory bulb output neurons. *J. Physiol.* 596, 2185–2207. doi: 10.1113/JP275511

Lukas, M., Suyama, H., and Egger, V. (2019). Vasopressin cells in the rodent olfactory bulb resemble non-bursting superficial tufted cells and are primarily inhibited upon olfactory nerve stimulation. *eNeuro* 6:2019. doi: 10.1523/ENEURO.0431-18.2019

Mctavish, T. S., Migliore, M., Shepherd, G. M., and Hines, M. L. (2012). Mitral cell spike synchrony modulated by dendrodendritic synapse location. *Front. Comput. Neurosci.* 6:3. doi: 10.3389/fncom.2012.00003

Nagayama, S., Homma, R., and Imamura, F. (2014). Neuronal organization of olfactory bulb circuits. *Front. Neural Circuits* 8:98. doi: 10.3389/fncir.2014.00098

Najac, M., De Saint Jan, D., Reguero, L., Grandes, P., and Charpak, S. (2011). Monosynaptic and polysynaptic feed-forward inputs to mitral cells from olfactory sensory neurons. *J. Neurosci.* 31, 8722–8729. doi: 10.1523/JNEUROSCI.0527-11.2011

Oettl, L. L., Ravi, N., Schneider, M., Scheller, M. F., Schneider, P., Mitre, M., et al. (2016). Oxytocin enhances social recognition by modulating cortical control of early olfactory processing. *Neuron* 90, 609–621. doi: 10.1016/j.neuron.2016.03.033

Osinski, B. L., and Kay, L. M. (2016). Granule cell excitability regulates gamma and beta oscillations in a model of the olfactory bulb dendrodendritic microcircuit. *J. Neurophysiol.* 116, 522–539. doi: 10.1152/jn.00988.2015

Ostrowski, N., Lolait, S., and Young, W. (1994). Cellular localization of vasopressin V1a receptor messenger ribonucleic acid in adult male rat brain, pineal, and brain vasculature. *Endocrinology* 135, 1511–1528. doi: 10.1210/endo.135.4.7925112

Pankevich, D. E., Baum, M. J., and Cherry, J. A. (2004). Olfactory sex discrimination persists, whereas the preference for urinary odorants from estrous females disappears in male mice after vomeronasal organ removal. *J. Neurosci.* 24, 9451–9457. doi: 10.1523/JNEUROSCI.2376-04.2004

Ramanathan, G., Cilz, N. I., Kurada, L., Hu, B., Wang, X., and Lei, S. (2012). Vasopressin facilitates Gabaergic transmission in rat hippocampus via activation of V1A receptors. *Neuropharmacology* 63, 1218–1226. doi: 10.1016/j.neuropharm.2012.07.043

Shao, Z., Puche, A. C., Kiyokage, E., Szabo, G., and Shipley, M. T. (2009). Two Gabaergic Intraglomerular circuits differentially regulate tonic and phasic presynaptic inhibition of olfactory nerve terminals. *J. Neurophysiol.* 101, 1988–2001. doi: 10.1152/jn.91116.2008

Shepherd, G. M., Chen, W. R., and Greer, C. A. (2004). "Olfactory bulb" in The synaptic organization of the brain. ed. G. M. Shepherd (Oxford: Oxford University Press).

Singer, A. G., Beauchamp, G. K., and Yamazaki, K. (1997). Volatile signals of the major histocompatibility complex in male mouse urine. *Proc. Natl. Acad. Sci. USA* 94, 2210–2214. doi: 10.1073/pnas.94.6.2210

Stark, R. (2024). The olfactory bulb: a neuroendocrine spotlight on feeding and metabolism. *J. Neuroendocrinol.* 36:e13382. doi: 10.1111/jne.13382

Stroh, O., Freichel, M., Kretz, O., Birnbaumer, L., Hartmann, J., and Egger, V. (2012). Nmda receptor-dependent synaptic activation of Trpc channels in olfactory bulb granule cells. *J. Neurosci.* 32, 5737–5746. doi: 10.1523/JNEUROSCI.3753-11.2012

Sun, C., Yin, Z., Li, B.-Z., Du, H., Tang, K., Liu, P., et al. (2021). Oxytocin modulates neural processing of mitral/tufted cells in the olfactory bulb. *Acta Physiol.*:e13626. doi: 10.1111/apha.13626

Suyama, H., Egger, V., and Lukas, M. (2021). Top-down acetylcholine signaling via olfactory bulb vasopressin cells contributes to social discrimination in rats. *Commun. Biol.* 4:603. doi: 10.1038/s42003-021-02129-7

Suyama, H., Egger, V., and Lukas, M. (2022). Mammalian social memory relies on neuromodulation in the olfactory bulb. *e-Neuroforum* 28, 143–150. doi: 10.1515/nf-2022-0004

Tada, M., Takeuchi, A., Hashizume, M., Kitamura, K., and Kano, M. (2014). A highly sensitive fluorescent indicator dye for calcium imaging of neural activity in vitro and in vivo. *Eur. J. Neurosci.* 39, 1720–1728. doi: 10.1111/ejn.12476

Tavakoli, A., Schmaltz, A., Schwarz, D., Margrie, T. W., Schaefer, A. T., and Kollo, M. (2018). Quantitative Association of Anatomical and Functional Classes of olfactory bulb neurons. *J. Neurosci.* 38, 7204–7220. doi: 10.1523/JNEUROSCI.0303-18.2018

Tobin, V. A., Hashimoto, H., Wacker, D. W., Takayanagi, Y., Langnaese, K., Caquineau, C., et al. (2010). An intrinsic vasopressin system in the olfactory bulb is involved in social recognition. *Nature* 464, 413–417. doi: 10.1038/nature08826

Urban, I. J. A., and Killian, M. J. P. (1990). Two actions of vasopressin on neurons in the rat ventral hippocampus: a microiontophoretic study. *Neuropeptides* 16, 83–90. doi: 10.1016/0143-4179(90)90116-G

Van Den Hooff, P., and Urban, I. J. A. (1990). Vasopressin facilitates excitatory transmission in slices of the rat dorso-lateral septum. *Synapse* 5, 201–206. doi: 10.1002/syn.890050305